



HAL
open science

A Simple RCS Calibration Approach For Depolarizing Chipless RFID Tags

Zeshan Ali, Etienne Perret

► **To cite this version:**

Zeshan Ali, Etienne Perret. A Simple RCS Calibration Approach For Depolarizing Chipless RFID Tags. 2021 IEEE/MTT-S International Microwave Symposium - IMS 2021, Jun 2021, Atlanta, United States. pp.165-168, 10.1109/ims19712.2021.9574947. hal-03413141

HAL Id: hal-03413141

<https://hal.science/hal-03413141>

Submitted on 5 Nov 2021

HAL is a multi-disciplinary open access archive for the deposit and dissemination of scientific research documents, whether they are published or not. The documents may come from teaching and research institutions in France or abroad, or from public or private research centers.

L'archive ouverte pluridisciplinaire **HAL**, est destinée au dépôt et à la diffusion de documents scientifiques de niveau recherche, publiés ou non, émanant des établissements d'enseignement et de recherche français ou étrangers, des laboratoires publics ou privés.

A Simple RCS Calibration Approach For Depolarizing Chipless RFID Tags

Zeshan Ali^{#1}, and Etienne Perret^{**2}

[#]Univ. Grenoble Alpes, Grenoble INP, LCIS, 26000 Valence, France

^{*}Institut Universitaire de France, 75005 Paris, France

¹zeshan.ali@lcis.grenoble-inp.fr, ²etienne.perret@lcis.grenoble-inp.fr

Abstract—A simple and convenient approach for the calibration of cross polarized radar cross section (RCS) is presented. We have shown that a planar depolarizing chipless radio frequency identification (RFID) tag can be utilized as a reference calibration target for the calibration, especially for the characterization of its counterpart depolarizing chipless RFID tags. To prove the concept, one chipless RFID tag is used as a reference calibration tag and another one as a test tag. The designs of chipless RFID tags are based on RF encoding particle (REP) and taken from the literature. The experimental performance of the proposed method is compared with the ideal simulated RCS. The worst calibration error over a frequency range from 4 to 7 GHz is less than 3.11 dB, whereas the worst calibration error over a frequency range from 4 to 6 GHz is less than 2.51 dB.

Keywords—chipless RFID, depolarizing scatterer, radar calibration, radar cross section, RCS magnitude coding.

I. INTRODUCTION

Recent advances have made it possible to consider the chipless radio frequency (RF) identification (RFID) as a significant counterpart to the well-known barcode [1]. For the frequency-coded chipless RFID tags, the identification (ID) is encoded in various features of the backscattered fingerprint. For example, the frequency position (FP) encoding (based on the peak apexes or the dips) is combined with: phase [2], group delay [3], [4], angle [5], bandwidth [6], polarization [7], dual-band and polarization [8], co polarized radar cross section (RCS) magnitude [9], and cross polarized RCS magnitude [10]. The co polarized RCS calibration for a chipless RFID tag can be done using one nondepolarizing reference object (e.g., rectangular metallic plate, metallic disk and metallic sphere) as discussed in [2], [9], [11]. On the other hand, precise calibration of cross polarized RCS is also needed to characterize and compare chipless RFID tag performance. It is the only way to obtain the tag intrinsic value characterizing the level of the backscattered power that is not dependent on the measurement bench (for instance the reader to tag distance) and so that can be used to compare different tags. Note that RCS is a physical quantity that is used to compute significant tag performance such as the reading distance. To the best of the authors' knowledge, none of the existing works has discussed cross polarized RCS calibration for chipless RFID in particular. One way is to perform full polarimetric radar calibration [12], [13] of chipless RFID system. These methods are proven and provide precise estimation of RCS. However, these methods are complex to implement and also require multiple reference

objects which may explain why they are not used in practice. These reference objects include nondepolarizing objects and depolarizing objects. The common depolarizing objects are corner reflectors (dihedral and trihedral), wire mesh, and cylinder [11]. These objects are bulky and 3D.

In this paper, a simple RCS calibration approach for depolarizing chipless RFID tags is presented. Here, the idea is to exploit the resonant signal with a limited number of frequencies for the wideband calibration. For this purpose, an extrapolation is carried out outside the resonance frequencies, which makes it possible with this new technique to carry out a wideband calibration. We have shown that a planar depolarizing chipless RFID tag can be utilized as a reference calibration scatterer for the calibration of its counterpart depolarizing chipless RFID tags. To prove the concept, one chipless RFID tags is used as a reference calibration target and another one as a test tag. This reference object is planar, low cost, and realized using a printed circuit board (PCB) in comparison to the conventional (possibly more accurate) 3D corner reflectors (dihedral and trihedral). Furthermore, the proposed calibration object is very promising for the chipless RFID industry, as the proposed calibration object (i.e., also a chipless RFID tag) is easy to use and readily available as compared to the other calibration objects. In the literature, such calibration of depolarizing objects is commonly done using a broadband target (not a resonant scatterer). Also, the proposed cross polarized RCS calibration is novel in comparison to the co polarized RCS calibration presented in [2], because it is for depolarizing chipless RFID tags. The experimental performance of the proposed RCS calibration object is compared with the simulated ideal RCS.

II. DESIGNS OF REFERENCE CALIBRATION AND TEST CHIPLESS RFID TAGS, AND THEIR SIMULATIONS

The purpose of this paper is to introduce a possible novel use of the chipless RFID tag as a reference calibration object (but not to introduce novel designs of tags). Therefore, the designs of the reference calibration and the test chipless RFID tags are taken from the literature [14]. The photographs of the reference calibration and the test chipless RFID tags are presented in Fig. 1. The reference calibration tag [Fig. 1(a)] is based on 45° shorted dipoles, whereas the test tag [Fig. 1(b)] is based on dual-L resonators. These tags were realized using PCB technology on a Rogers RO4003C substrate with substrate height $h = 0.81$ mm and dielectric permittivity $\epsilon_r = 3.55$ [14]. The geometrical dimensions of both the reference calibration

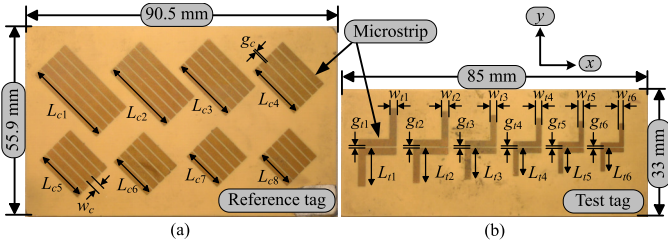


Fig. 1. Photographs of chipless RFID tags. (a) Reference calibration tag based on 45° shorted dipoles. (b) Test tag based on dual-L resonators.

Table 1. Geometrical dimensions (in mm) of chipless RFID tags.

Tags	Parameters ^a	Scatterers							
		1	2	3	4	5	6	7	8
Reference	L_{ri}	24.8	21.8	19	16.8	15	13.4	12.2	11.2
Test	L_{ti}	10.9	10	9	8.1	7.3	6.75		
	w_{ti}	1.99	1.83	1.64	1.47	1.33	1.23		
	g_{ti}	0.5	0.45	0.41	0.37	0.33	0.31		

^a L_{ri} , the length of each scatterer of the reference calibration tag; L_{ti} , the length of each L-shaped resonator of the test tag; w_{ti} , the width of the microstrip trace of each resonator of the test tag; g_{ti} , the space between dual-L coupled resonators of the test tag.

and the test tags are provided in Table 1 to facilitate the reproduction for the reader. Additionally, for the reference calibration tag, the microstrip trace width is $w_c = 2$ mm and the space between multiple coupled dipoles is $g_c = 0.5$ mm. The overall size dimensions of the reference calibration tag and the test tag are 90.5×55.9 mm² and 85×33 mm², respectively.

The ideal RCS signals of the chipless RFID tags are estimated using the computer simulations with a commercial full-wave simulator (CST Microwave Studio). Fig. 2 shows the CST estimated cross polarized RCS signal of reference calibration tag σ_{21}^{ref} . Such σ_{21}^{ref} signal might not be directly utilized in the calibration procedure, because of the resonant behaviour of the reference calibration tag. Merely the peak apexes present the acceptable level of signal to noise ratio (SNR). Otherwise of these peak apexes, the backscattered SNR is too low. For this reason, the peak apexes of σ_{21}^{ref} are detected and a spline fit signal $\sigma_{21}^{\text{ref-fit}}$ is calculated. This $\sigma_{21}^{\text{ref-fit}}$ will be used in the broadband calibration procedure next in this paper.

III. CALIBRATION PROCEDURE, RESULTS AND COMPARISON

The experimental measurements are performed using a single antenna-based monostatic radar configuration inside the anechoic environment as shown in Fig. 3. For this purpose, vertical (V) and horizontal (H) polarized ports of the Satimo QH2000 dual polarization horn antenna (2–32 GHz) are connected to port 1 and port 2 of Agilent N5222A vector network analyzer (VNA), respectively, with an output power of -5 dBm. The frequency sweep ranging from 2 to 8 GHz with 10001 points is used. The isolation between ports of the antenna is greater than 30 dB. The distance between the tag and the antenna is $d = [10, 30]$ cm. The measured quantity is the transmission coefficient S_{21} . With $d = 10$ cm, the radar system is operating in the reactive nearfield and Fresnel zone

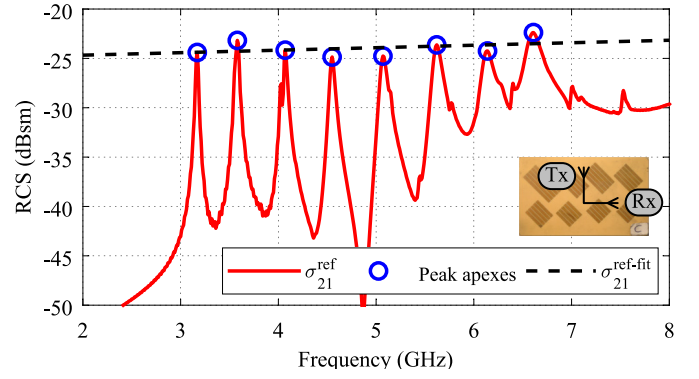


Fig. 2. Simulated cross polarized RCS signal of the reference calibration tag σ_{21}^{ref} along with its fit signal $\sigma_{21}^{\text{ref-fit}}$. Inset: corresponding photograph of the reference calibration tag.

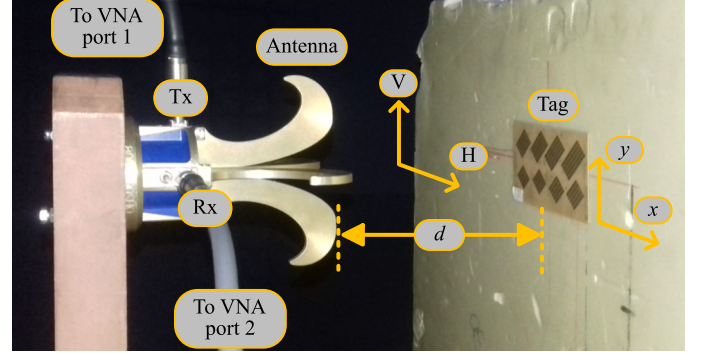


Fig. 3. Photograph of measurement setup inside an anechoic chamber.

for 2 GHz and 8 GHz, respectively. On the other hand, with $d = 30$ cm, the radar system is operating Fresnel zone over the whole frequency sweep (2 to 8 GHz). It is important to note that all measured signals are background normalized (i.e., the clutter is removed). Fig. 4 presents the measured S_{21} signals of the reference calibration tag for $d = 10$ cm $S_{21}^{\text{ref}(10\text{ cm})}$ along with its fit signal $S_{21}^{\text{ref-fit}(10\text{ cm})}$ [Fig. 4(a)] and for $d = 30$ cm $S_{21}^{\text{ref}(30\text{ cm})}$ along with its fit signal $S_{21}^{\text{ref-fit}(30\text{ cm})}$ [Fig. 4(b)]. The fit signals will be used in the calibration process. Fig. 5 presents the measured S_{21} signals of the test tag measured at $d = 10$ cm $S_{21}^{\text{tag}(10\text{ cm})}$ and $d = 30$ cm $S_{21}^{\text{tag}(30\text{ cm})}$. It should be noted from Figs. 4 and 5 that the reference calibration tag and the test tag do not present the same values of the frequencies of resonances.

The calibrated RCS of the test tag σ_{21}^{tag} is calculated using a simple and well-known formula [2]:

$$\sigma_{21}^{\text{tag}} = \left[\frac{S_{21}^{\text{tag}}}{S_{21}^{\text{ref-fit}}} \right]^2 \cdot \sigma_{21}^{\text{ref-fit}}. \quad (1)$$

It is important to mention here again that all measured signals are background normalized. For the calibration of the signals measured at $d = 10$ cm, $S_{21}^{\text{tag}} = S_{21}^{\text{tag}(10\text{ cm})}$ and $S_{21}^{\text{ref-fit}} = S_{21}^{\text{ref-fit}(10\text{ cm})}$ in (1). Whereas, for the calibration of the signals measured at $d = 30$ cm, $S_{21}^{\text{tag}} = S_{21}^{\text{tag}(30\text{ cm})}$ and $S_{21}^{\text{ref-fit}} = S_{21}^{\text{ref-fit}(30\text{ cm})}$ in (1). Fig. 6 shows the calibrated cross polarized RCS signal of the test tag σ_{21}^{tag} measured at $d = 10$ cm

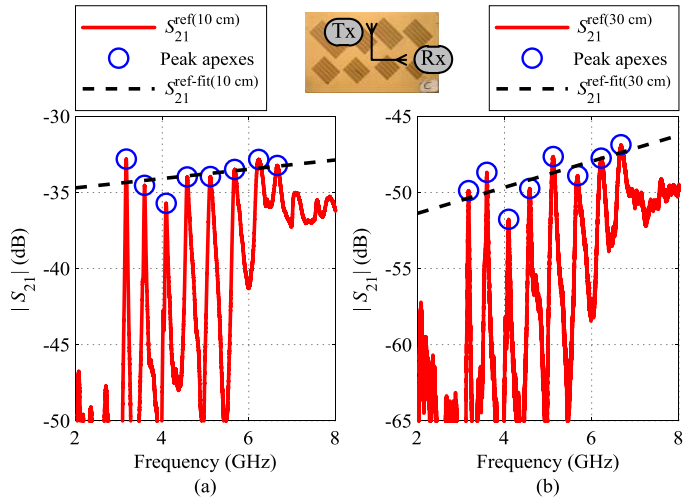


Fig. 4. Measured S_{21} signals of the reference calibration tag along with their fit signals using the peak apexes. (a) $S_{21}^{\text{ref}(10 \text{ cm})}$ along with its fit signal $S_{21}^{\text{ref-fit}(10 \text{ cm})}$. (b) $S_{21}^{\text{ref}(30 \text{ cm})}$ along with its fit signal $S_{21}^{\text{ref-fit}(30 \text{ cm})}$. Inset: corresponding photograph of the reference calibration tag.

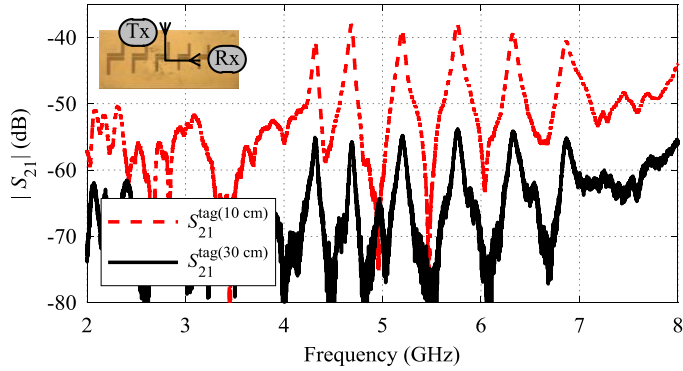


Fig. 5. Measured S_{21} signals of the test tag measured at $d = 10 \text{ cm}$ $S_{21}^{\text{tag}(10 \text{ cm})}$ and at $d = 30 \text{ cm}$ $S_{21}^{\text{tag}(30 \text{ cm})}$. Inset: corresponding photograph of the test tag.

$\sigma_{21}^{\text{tag}(10 \text{ cm})}$ and at $d = 30 \text{ cm}$ $\sigma_{21}^{\text{tag}(30 \text{ cm})}$ in comparison with the CST estimated cross polarized RCS signal $\sigma_{21}^{\text{tag-CST}}$. It can be observed that both $\sigma_{21}^{\text{tag}(10 \text{ cm})}$ and $\sigma_{21}^{\text{tag}(30 \text{ cm})}$ present a good match with the CST estimated cross polarized RCS of the test tag $\sigma_{21}^{\text{tag-CST}}$.

The peak-to-peak calibration error is calculated as $\Delta\sigma_{21}^{\text{tag}} = \sigma_{21}^{\text{tag-CST}} - \sigma_{21}^{\text{tag}}$. Fig. 7 presents $\Delta\sigma_{21}^{\text{tag}}$ for the experimental measurements performed at $d = 10 \text{ cm}$ $\Delta\sigma_{21}^{\text{tag}(10 \text{ cm})}$ and at $d = 30 \text{ cm}$ $\Delta\sigma_{21}^{\text{tag}(30 \text{ cm})}$. It can be observed that within the frequency range from 4 to 6 GHz, $\Delta\sigma_{21}^{\text{tag}(10 \text{ cm})} < 1.59 \text{ dB}$ and $\Delta\sigma_{21}^{\text{tag}(30 \text{ cm})} < 2.51 \text{ dB}$. On the other hand, for the frequency range from 4 to 7 GHz, $\Delta\sigma_{21}^{\text{tag}(10 \text{ cm})} < 2.65 \text{ dB}$ and $\Delta\sigma_{21}^{\text{tag}(30 \text{ cm})} < 3.11 \text{ dB}$.

The employed reference calibration chipless RFID tag (i.e., based on 45° shorted dipoles) was not designed for the calibration purpose. The obtained peak-to-peak calibration errors might be reduced by designing a reference chipless RFID tag specifically for the calibration purpose.

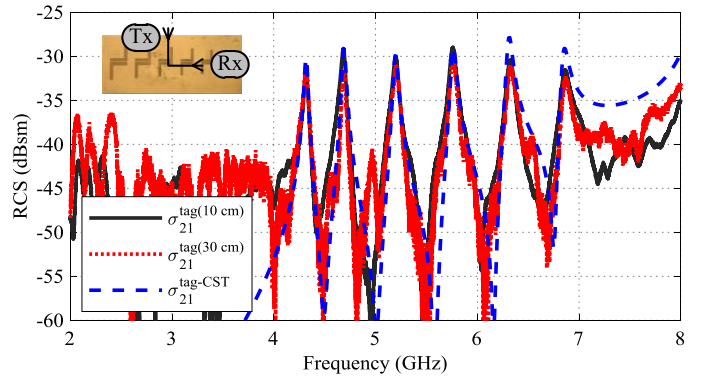


Fig. 6. Calibrated cross polarized RCS signal of test tag S_{21}^{tag} measured at $d = 10 \text{ cm}$ $\sigma_{21}^{\text{tag}(10 \text{ cm})}$ and at $d = 30 \text{ cm}$ $\sigma_{21}^{\text{tag}(30 \text{ cm})}$ in comparison with the CST estimated cross polarized RCS signal $\sigma_{21}^{\text{tag-CST}}$.

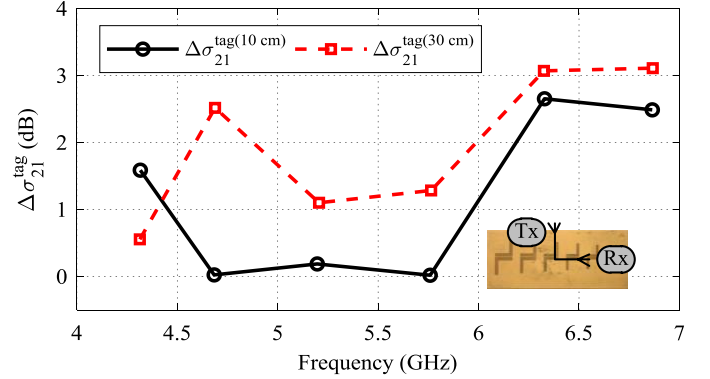


Fig. 7. Peak-to-peak calibration error $\Delta\sigma_{21}^{\text{tag}(10 \text{ cm})}$ and $\Delta\sigma_{21}^{\text{tag}(30 \text{ cm})}$. Inset: corresponding photograph of the test tag.

IV. CONCLUSION

In this paper, a possible novel use of a depolarizing chipless RFID tag to be utilized for the calibration of its counterpart depolarizing chipless RFID tags was introduced. The concept was proved by considering one chipless RFID tag as a reference calibration tag and another as a test tag. Firstly, the proposed approach is general and not limited to chipless tag characterization only. Secondly, more accurate models or approaches compared to (1) (available in the literature) can be used to improve the accuracy of the use of chipless tag as a depolarizing target. The employed calibration reference object is a planar and low cost PCB circuit in comparison to 3D corner reflectors. Furthermore, the proposed calibration object is very promising for chipless RFID industry, as the employed chipless RFID tag as a reference calibration object is easy to use and readily available as compared to the other calibration objects. The performance of the proposed method is compared with the CST simulated ideal RCS. The worst calibration error over a frequency range from 4 to 7 GHz is less than 3.11 dB.

ACKNOWLEDGMENT

This work is funded by the European Research Council (ERC) under the European Union's Horizon 2020 research and innovation program under grant agreement no. 772539 (SCATTERERID, <https://www.scattererid.eu/>).

REFERENCES

- [1] E. Perret, *Radio Frequency Identification and Sensors: From RFID to Chipless RFID*. Hoboken, NJ, USA: Wiley, 2014.
- [2] A. Vena, E. Perret, and S. Tedjini, "Chipless RFID Tag Using Hybrid Coding Technique," *IEEE Trans. Microw. Theory Techn.*, vol. 59, no. 12, pp. 3356–3364, Dec. 2011.
- [3] R. S. Nair and E. Perret, "Folded Multilayer C-Sections With Large Group Delay Swing for Passive Chipless RFID Applications," *IEEE Trans. Microw. Theory Techn.*, vol. 64, no. 12, pp. 4298–4311, Dec. 2016.
- [4] S. Gupta, B. Nikfal, and C. Caloz, "Chipless RFID System Based on Group Delay Engineered Dispersive Delay Structures," *IEEE Antennas Wireless Propag. Lett.*, vol. 10, pp. 1366–1368, 2011.
- [5] C. Feng, W. Zhang, L. Li, L. Han, X. Chen, and R. Ma, "Angle-Based Chipless RFID Tag With High Capacity and Insensitivity to Polarization," *IEEE Trans. Antennas Propag.*, vol. 63, no. 4, pp. 1789–1797, Apr. 2015.
- [6] A. El-Awamry, M. Khaliel, A. Fawky, M. El-Hadidy, and T. Kaiser, "Novel notch modulation algorithm for enhancing the chipless RFID tags coding capacity," in *Proc. IEEE Int. Conf. RFID*, San Diego, CA, USA, Apr. 2015, pp. 25–31.
- [7] M. Khaliel, A. El-Awamry, A. Fawky Megahed, and T. Kaiser, "A Novel Design Approach for Co/Cross-Polarizing Chipless RFID Tags of High Coding Capacity," *IEEE J. Radio Freq. Identif.*, vol. 1, no. 2, pp. 135–143, Jun. 2017.
- [8] F. Babaeian and N. C. Karmakar, "Hybrid Chipless RFID Tags- A Pathway to EPC Global Standard," *IEEE Access*, vol. 6, pp. 67 415–67 426, 2018.
- [9] Y. Ni, X. Huang, Y. Lv, and C. Cheng, "Hybrid coding chipless tag based on impedance loading," *IET Microw. Antennas Propag.*, vol. 11, no. 10, pp. 1325–1331, Aug. 2017.
- [10] O. Rance, E. Perret, R. Siragusa, and P. Lemaitre-Auger, *RCS Synthesis for Chipless RFID: Theory and Design*. Amsterdam, The Netherlands: Elsevier, 2017.
- [11] W. Wiesbeck and D. Kahny, "Single reference, three target calibration and error correction for monostatic, polarimetric free space measurements," *Proc. IEEE*, vol. 79, no. 10, pp. 1551–1558, Oct. 1991.
- [12] M. W. Whitt, F. T. Ulaby, P. Polatin, and V. V. Liepa, "A general polarimetric radar calibration technique," *IEEE Trans. Antennas Propag.*, vol. 39, no. 1, pp. 62–67, 1991.
- [13] B. M. Welsh, B. M. Kent, and A. L. Buterbaugh, "Full polarimetric calibration for radar cross-section measurements: performance analysis," *IEEE Trans. Antennas Propag.*, vol. 52, no. 9, pp. 2357–2365, 2004.
- [14] A. Vena, E. Perret, and S. Tedjini, "A Depolarizing Chipless RFID Tag for Robust Detection and Its FCC Compliant UWB Reading System," *IEEE Trans. Microw. Theory Techn.*, vol. 61, no. 8, pp. 2982–2994, Aug. 2013.